J. Biochem. 2009;145(1)103–113
doi:10.1093/jb/mvn140

Insights into the Catalytic Roles of the Polypeptide Regions in the Active Site of Thermolysin and Generation of the Thermolysin Variants with High Activity and Stability

Masayuki Kusano, Kiyoshi Yasukawa and Kuniyo Inouye*

Division of Food Science and Biotechnology, Graduate School of Agriculture, Kyoto University, Sakyo-ku, Kyoto 606-8502, Japan

Received September 6, 2008; accepted October 22, 2008; published online October 30, 2008

The active site of thermolysin is composed of one zinc ion and five polypeptide regions [N-terminal sheet (Asn112–Trp115), α-helix 1 (Val139–Thr149), C-terminal loop 1 (Asp150–Gly162), α-helix 2 (Ala163–Val176) and C-terminal loop 2 (Gln225–Ser234)]. To explore their catalytic roles, we introduced single amino-acid substitutions into these regions by site-directed mutagenesis and examined their effects on the activity and stability. Seventy variants, in which one of the twelve residues (Ala113, Phe114, Trp115, Asp150, Tyr157, Gly162, Ile168, Ser169, Asp170, Asn227, Val230 and Ser234) was replaced, were produced in *Escherichia coli*. The hydrolytic activities of thermolysin for *N*-[3-(2-furyl)acryloyl]-Gly-L-Leu amide (FAGLA) and casein revealed that the N-terminal sheet and α-helix 2 were critical in catalysis and the C-terminal loops 1 and 2 were in substrate recognition. Twelve variants were active for both substrates. In the hydrolysis of FAGLA and *N*-carbobenzoxy-L-Asp-L-Phe methyl ester, the k_{cat}/K_m values of the D150E (in which Asp150 is replaced with Glu) and I168A variants were 2–3 times higher than those of the wild-type (WT) enzyme. Thermal inactivation of thermolysin at 80°C was greatly suppressed with the D150H, D150W, I168A, I168H, N227A, N227H and S234A. The evidence might provide the insights into the activation and stabilization of thermolysin.

Key words: active site, metalloproteinase, site-directed mutagenesis, stability, thermolysin.

Abbreviations: FAGLA, *N*-[3-(2-furyl)acryloyl]-glycyl-L-leucine amide; ZDFM, *N*-carbobenzoxy-L-aspartyl-L-phenylalanine methyl ester.

INTRODUCTION

Thermolysin [EC 3.4.24.27] is a thermostable neutral metalloproteinase produced in the culture broth of *Bacillus thermoproteolyticus* (*1–3*). It requires one zinc ion for enzyme activity and four calcium ions for structural stability (*4–6*), and catalyses specifically the hydrolysis of peptide bonds containing hydrophobic amino acid residues (*7*, *8*). Thermolysin consists of 316 amino acid residues, and the amino acid sequence was determined (*9*). Based on the structural data (*10–12*), thermolysin consists of a β-rich N-terminal domain and an α-helical C-terminal domain.

Thermolysin is widely used for the peptide bond formation through reverse reaction of hydrolysis, in particular *N*-carbobenzoxy-L-aspartyl-L-phenylalanine methyl ester (ZDFM), a precursor of an artificial sweetener aspartame, from *N*-carbobenzoxy-L-aspartic acid (ZD) and L-phenylalanine methyl ester (FM) (*13*, *14*). Therefore, the improvement of its activity and stability and the modification of its pH-activity profile are important subjects (*15*). For example, the ZDFM synthesis by thermolysin is carried out at pH 5–6 to prevent the hydrolysis of the methylester of FM and ZDFM, while the optimum pH of thermolysin activity is around 7 (*16*). We have examined the effects of the solvent composition on the activity and stability of thermolysin, and have reported the remarkable activation (*8*, *14*, *17–20*) and stabilization (*17*) by high concentrations of neutral salts. Thermolysin activity increases in an exponential fashion with increasing salt concentration (*8*, *14*, *19*, *20*). Accordingly, we have defined thermolysin as the most representative halophilic and thermophilic enzyme (*17*, *18*). Site-directed mutagenesis experiments of thermolysin have generated a number of variants with improved activity and/or stability. The L144S, D150W and N227H variants (in which the active-site residues Leu144, Asp150 and Asn227 are replaced with Ser, Trp and His, respectively) were improved in thermolysin activity (*16*, *21*); the G8C/N60C/S65P variant (Gly8, Asn60 and Ser65 in the N-terminal region are replaced with Cys, Cys and Pro, respectively, to introduce a disulfide bridge between the positions 8 and 60) (*21*), the L155A variant (the autodegradation-site residue Leu155 in the active site is replaced with Ala) (*22*, *23*) and the S53D variant (Ser53 in the N-terminal region is replaced with Asp to stabilize the Ca^{2+} ion) (*24*) were improved in stability; the G8C/N60C/S65P/L144S variant (*21*) was improved in both activity and stability; the N112D (the active-site residue Asn112 is replaced with Asp) (*25*) and Q225A variants

*To whom correspondence should be addressed. Tel: +81-75-753-6266, Fax: +81-75-753-6265, E-mail: inouye@kais.kyoto-u.ac.jp

© The Authors 2008. Published by Oxford University Press on behalf of the Japanese Biochemical Society. All rights reserved.

Downloaded from http://jb.oxfordjournals.org/ at University of Science and Technology of China on September 28, 2012

(the active-site surface residue Gln225 is replaced with Ala) (*26*) were modified in the pH-activity profile. One of the obstacles of the site-directed mutagenesis study of thermolysin is that thermolysin is produced as pre-proenzyme (*27*, *28*), and thus thermolysin variants cannot be produced if they lose the autocatalytic digestion activity. Actually, the N112A, N112K, N112H and N112R variants were not produced in the conventional *Escherichia coli* expression method (*25*). It was revealed that this obstacle was overcome by expressing the mature sequence and pro-sequence of thermolysin in *E. coli* as independent polypeptides (*29*).

The active site of thermolysin is composed of five polypeptide regions (hereinafter named N-terminal sheet, α-helices 1 and 2, and C-terminal loops 1 and 2) and they form a deep cleft (Fig. 1). The α-helix 1 contains the zinc-binding consensus sequence $H^{142}EXXH^{146}$ and connects the N- and C-terminal domains. Glu143 is a candidate for the ionizable residue responsible for the pK_a value observed in the acidic side of the bell-shaped pH-dependence curve of the activity, k_{cat}/K_m (*8*, *18*) and both His142 and His146 chelate the active-site zinc ion. In order to explore the catalytic roles of the four polypeptide regions other than the α-helix 1, three residues were selected from each region and replaced with Ala, Asp, Glu, His, Lys and Arg. The thermolysin variants thus designed were expressed in *E. coli* and characterized for catalytic activities and thermal stabilities in the hydrolysis of casein, *N*-[3-(2-furyl)acryloyl]-glycyl-L-leucine amide (FAGLA), a widely used substrate for thermolysin (*14*, *30*) and ZDFM (*13*, *14*).

MATERIALS AND METHODS

Materials—Casein (Lot WKL1761) was purchased from Wako Pure Chemical (Osaka, Japan). FAGLA (Lot 111K1764) was purchased from Sigma (St Louis, MO). The concentration of FAGLA was determined spectrophotometrically using the molar absorption coefficient, $\varepsilon_{345} = 766\,M^{-1}cm^{-1}$ (*14*, *30*). ZDFM was prepared as described previously (*14*). The concentration of ZDFM was determined using the molar absorption coefficient, $\varepsilon_{257} = 387\,M^{-1}cm^{-1}$ (*14*).

Bacterial Strains, Plasmids and Transformation—*E. coli* K12 JM109 [*recA1, endA1, gyrA96, thi, hsdR17, supE44, relA1, Δ*(*lac-proAB*), *F′*(*traD36, proAB*$^+$ *lac*^{Iq}, *lacZΔM15*)] was used. pTMP1 is an expression plasmid that co-expresses the mature sequence of thermolysin containing the pelB leader sequence at its N-terminus and the pre-prosequence of thermolysin, as described previously (*29*). Site-directed mutagenesis was carried out using a Quikchange™ site-directed mutagenesis kit (Stratagene, La Jolla, CA). The nucleotide sequences of mutated thermolysin genes were verified by a Shimadzu DNA sequencer DSQ-2000 (Kyoto, Japan). JM109 cells were transformed with each of the resulted plasmids and cultured in L broth. Ampicillin was used at the concentration of 50 μg/ml.

Characterization of Thermolysins in the Culture Supernatants—For seed culture, 5 ml of L broth in a 20 ml test tube was inoculated with the glycerol stock of the transformed JM109 cells and grown with shaking at 37°C for 12 h. The culture (0.05 ml) was diluted 100 times with 5 ml of L broth in a 20 ml test tube and grown with shaking at 37°C for 48 h. The supernatant was collected by the centrifugation at 20,400 × *g* for 3 min at 4°C and was subjected to SDS–PAGE and the hydrolysis of casein and FAGLA.

Production of Thermolysin Variants—Production of thermolysin was performed as described earlier (*28*, *29*, *31*). Briefly, for seed culture, 5 ml of L broth in a 20 ml test tube was inoculated with the glycerol stock of the transformed JM109 cells and grown with shaking at 37°C for 12 h. The culture (5 ml) was diluted 100 times with 500 ml of L broth in a 1 l flask and incubated under the conditions at 37°C for 48 h, with 0.1% (w/v) anti-form A (Sigma) and vigorous aeration by an air-pump. The variants were purified to homogeneity by sequential column-chromatography procedures of the supernatant of *E. coli* cultures with hydrophobic-interaction chromatography followed by affinity chromatography. Prior to kinetic measurements, the preparations were desalted using pre-packed PD-10 gel filtration columns (Amersham Biosciences, Uppsala, Sweden).

SDS–PAGE—SDS–PAGE was performed in a 12.5% polyacrylamide gel under reducing conditions according to the method of Laemmli (*32*). A constant current of 40 mA was applied for 40 min. Supernatants were reduced by treatment with 2.5% 2-mercaptoethanol at 100°C for 10 min. Proteins were stained with Coomassie Brilliant Blue R-250. The molecular-mass marker kit consisting of rabbit muscle phosphorylase *b* (97.4 kDa), bovine serum albumin (66.3 kDa), rabbit muscle aldolase (42.4 kDa), bovine erythrocyte carbonic anhydrase (30.0 kDa), soybean trypsin inhibitor (20.1 kDa) and hen egg-white lysozyme (14.4 kDa) was a product of Daiichi Pure Chemicals (Tokyo, Japan).

Hydrolysis of Casein—The casein-hydrolyzing activity was determined according to the methods described previously (*3*, *26*). The thermolysin solution (0.5 ml) were added to 1.5 ml of a solution containing 1.33% (w/v) casein and 40 mM Tris–HCl (pH 7.5) and incubated at 25°C for 30 min. The reaction was stopped by the addition of 2 ml of a solution containing 0.11 M trichloroacetic acid, 0.22 M sodium acetate and 0.33 M acetic acid. After 1 h incubation at 25°C, the reaction mixture was filtered through Whatman No. 2 filter paper (70 mm in diameter) and the absorbance (A_{275}) at 275 nm was measured. One proteolytic unit (PU) of activity is defined as the amount of enzyme activity needed to liberate a quantity of acid soluble peptides corresponding to an increase in A_{275} of 0.0074 (A_{275} of 1 μg of tyrosine)/min.

Spectrophotometric Analysis of the Thermolysin-Catalysed Hydrolysis of FAGLA—The thermolysin-catalysed hydrolysis of FAGLA was measured following the decrease in absorbance (A_{345}) at 345 nm (*8*, *14*). The amount of FAGLA hydrolysed was evaluated using the molar absorption difference due to hydrolysis, $\Delta\varepsilon_{345} = -310\,M^{-1}cm^{-1}$, at 25°C (*8*, *14*, *30*). The reaction was carried out in 40 mM acetate–NaOH buffer at pH 4.0–5.5, 40 mM MES–NaOH buffer at pH 5.5–7.0, 40 mM HEPES–NaOH buffer at pH 7.0–8.5 and TAPS–NaOH buffer at pH 8.0–9.0, each of which containing 10 mM $CaCl_2$, at 25°C. The hydrolysis was carried out under

Downloaded from http://jb.oxfordjournals.org/ at University of Science and Technology of China on September 28, 2012

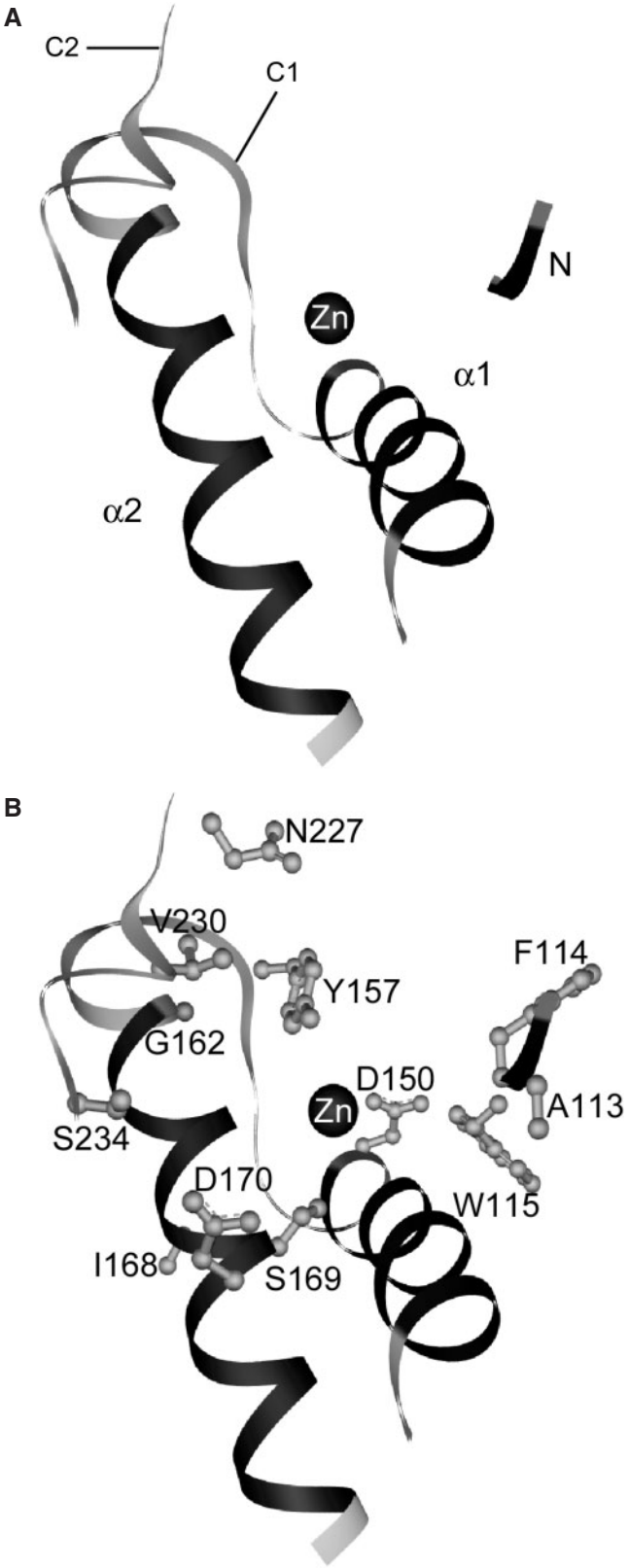

Fig. 1. **Close-up view of the active site of thermolysin.** The structure is based on Protein Data Bank number 8TLN (*37*). Protein is displayed by flat ribbon. (A) Five active-site regions. N, α1, C1, α2 and C2 denote the N-terminal sheet (Asn112–Trp115), the α-helix 1 (Val139–Thr149), the C-terminal loop 1 (Asp150–Gly162), the α-helix 2 (Ala163–Val176) and the C-terminal loop 2 (Gln225–Ser234), respectively. (B) Mutated amino-acid residues. The mutated amino-acid residues are displayed ball and stick. Distances from the C_α to the active-site zinc ion (Å): Ala113, 8.6; Phe114, 6.9; Trp115, 7.9; Asp150, 11.7; Tyr157, 9.4; Gly162, 9.2; Ile168, 8.6; Ser169, 5.9; Asp170, 7.5; Asn227, 11.9; Val230, 8.6 and Ser234, 9.9.

pseudo-first-order conditions, where the substrate concentration is much lower than the Michaelis constant (K_m) (>30 mM) (*14*) because of the sparing solubility (<6 mM) of FAGLA (*8*, *14*, *30*). Under the conditions, the kinetic parameters, K_m and the molecular activity (k_{cat}), cannot be determined separately and the enzyme activity was evaluated by the specificity constant (k_{cat}/K_m). The intrinsic k_{cat}/K_m [$(k_{cat}/K_m)_o$] and the proton dissociation constants (K_{e1} and K_{e2}) for the bell-shaped pH-dependence of the activity (k_{cat}/K_m) were calculated from Eq. 1 by a non-linear least-squares regression method with Kaleida Graph Version 3.5 (Synergy Software, Essex, VT).

$$\left(\frac{k_{cat}}{K_m}\right)_{obs} = \frac{(k_{cat}/K_m)_0}{\{1 + ([H]/K_{e1}) + (K_{e2}/[H])\}} \quad (1)$$

In this equation, $(k_{cat}/K_m)_{obs}$ and [H] mean the k_{cat}/K_m value observed and the proton concentration, respectively, at a specified pH, and K_{e1} and K_{e2} correspond to the pK_a's in the acidic and alkaline sides of the pH-dependence curve of $(k_{cat}/K_m)_{obs}$.

Spectrophotometric Analysis of the Thermolysin-Catalysed Hydrolysis of ZDFM—Thermolysin-catalysed hydrolysis of ZDFM was measured by following the decrease in absorbance (A_{224}) at 224 nm (*14*). The amount of ZDFM hydrolysed was evaluated using the molar absorption difference due to hydrolysis, $\Delta\varepsilon_{224} = -493\ M^{-1}cm^{-1}$, at 25°C (*14*). The reaction was carried out with thermolysin in 40 mM Tris–HCl (pH 7.5) buffer containing 10 mM $CaCl_2$ at 25°C. The kinetic parameters, k_{cat} and K_m, were determined with Kaleida Graph Version 3.5, based on the Michaelis-Menten equation using the non-linear least-squares methods (*33*).

Thermal Inactivation of Thermolysin—Thermolysin (0.5–8 μM) in 40 mM HEPES–NaOH (pH 7.5) buffer containing 10 mM $CaCl_2$ was incubated at 80°C for a specified time. Then, it was incubated at 25°C for 1 min. The remaining activity of the thermolysin toward FAGLA hydrolysis was determined as described above. Assuming that the thermal inactivation of thermolysin is irreversible and consists of only one step (*34*), the first-order rate constant, k_{obs}, of the thermal inactivation was evaluated by plotting logarithm of the residual activity (k_{cat}/K_m) against the time of thermal treatment.

RESULTS

Design of Thermolysin Variants—To explore the catalytic role of the N-terminal sheet, the α-helix 2 and the C-terminal loops 1 and 2 at the active site of thermolysin, we selected three residues to be mutated from each of the four regions, based on the criteria that the C_α atoms locate <12 Å far from the active-site zinc ion (Fig. 1). Glu166 and His231 were excluded from the selection because the former chelates the active-site zinc ion and the latter is

Downloaded from http://jb.oxfordjournals.org/ at University of Science and Technology of China on September 28, 2012

thought to be the ionizable residue responsible for the pK_{e2} of the pH-dependence of the activity (*2*, *3*, *15*). The twelve residues thus selected were changed into either one of negatively charged amino acids (Asp or Glu), positively charged ones (His, Lys or Arg), or an uncharged one (Ala). This strategy is based on our previous evidences that the mutation Ser53→Asp enhanced the thermal stability presumably by stabilizing the surface loop region through electrostatic interaction between the introduced Asp53 and Lys45 (*24*) and that the mutation Asn112→Asp shift the optimal pH to the alkaline side presumably by stabilizing the protonation of the ionizing residue responsible for pK_{e1} (*25*). We anticipated that this strategy might not only unveil the catalytic role of each polypeptide region in the active site of thermolysin but also generate some variants which are improved in activity and/or stability or modified in the pH-activity profile. The thermolysin D150W variant, which was previously shown to be more active than the wild-type (WT) thermolysin (*16*), was also constructed for comparison.

Characterization of the 70 Thermolysin Variants Using the Culture Supernatants of the E. coli Transformants—*E. coli* cells were transformed with the expression plasmids for WT thermolysin and its 70 variants. Each transformant was cultured in a test tube and harvested. The culture supernatants were first analysed by SDS–PAGE. The results with Ala113 variants showed that the 34 kDa protein band corresponding to the mature thermolysin was detected for all variants (Fig. 2A). The expression levels of most of the variants were comparable to that of the WT enzyme, but those with the mutations at the positions of 162, 168, 169 and 170 were substantially reduced (data not shown).

Table 1 shows the hydrolytic activities for casein and FAGLA of the thermolysin in the culture supernatants. Neither of the activities was detected for most of the variants with the mutation at the N-terminal sheet and the α-helix 2 (15 out of 17 and 14 out of 17, respectively). On the other hand, the activity only for casein was detected for considerable numbers of variants with the mutation at the C-terminal loops 1 and 2 (7 out of 18 and 8 out of 18, respectively). Therefore, it was suggested that the N-terminal sheet and the α-helix 2 might be critical in catalysis, while the C-terminal loops 1 and 2 were important in substrate specificity. As for the variants lacking the activity, the possibility that they might be impaired in folding into the active form due to the mutation introduced could not be eliminated. The effect of the mutation on the thermolysin folding should be examined precisely, although we selected the variants which have activity to subject them to analyse the relationship of the mutation with the activity and stability of thermolysin.

Production of 12 Thermolysin Variants to Homogeneity—For further characterization, twelve thermolysin variants (F114A, F114H, D150A, D150E, D150H, D150W, I168A, I168H, S169A, N227A, N227H and S234A) out of the 70 variants which retained hydrolytic activities for both FAGLA and casein were produced in the *E. coli* expression system (*29*). Starting from 350–400 ml of culture supernatants, the yields of the purified enzyme variants were in the range of 0.2–2.7 mg, less than or comparable to that (2.4 mg) of WT thermolysin. The SDS–PAGE pattern of the F114A variant at each purification stage is shown, as an example, in Fig. 2B. The purified F114A variant yielded a single band with a molecular mass of 34 kDa. The purities of other variants were almost the same as that of F114A (data not shown). CD spectra of

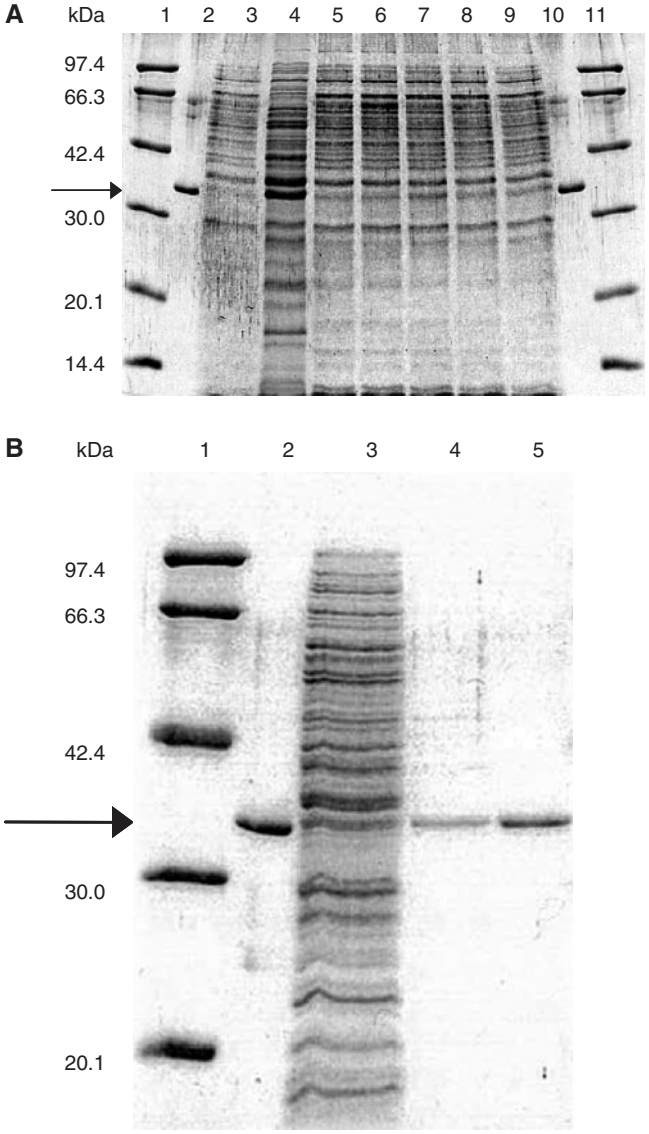

Fig. 2. **Coomassie Brilliant Blue-stained 12.5% SDS-polyacrylamide gels. (A) Expression of thermolysin variants**. The marker proteins (lanes 1 and 11), native thermolysin purified from *B. thermoproteolyticus* (lanes 2 and 10), the supernatants of *E. coli* cells transformed with pUC19 (lane 3), the expression plasmid for wild-type thermolysin (lane 4), A113D (lane 5), A113E (lane 6), A113H (lane 7), A113K (lane 8), and A113R (lane 9). (B) Purification of thermolysin variants. The marker proteins (lane 1), native thermolysin purified from *B. thermoproteolyticus* (lane 2), the supernatant of *E. coli* cells transformed with the expression plasmid for F114A (lane 3), active fractions of hydrophobic-interaction chromatography (lane 4), and active fractions of Gly-D-Phe affinity chromatography, which is purified F114A variant (lane 5). The arrow indicates the band corresponding to mature thermolysin.

Downloaded from http://jb.oxfordjournals.org/ at University of Science and Technology of China on September 28, 2012

Table 1. **Casein- and FAGLA-hydrolytic activities at 25°C of the culture supernatant of *E. coli* transformants expressing thermolysins.**

	Activity			Activity			Activity			Activity	
	C[a]	F[b]		C	F		C	F		C	F
Wild-type	100	100									
a. N-terminal sheet			b. α-helix 2			c. C-terminal loop 1			d. C-terminal loop 2		
A113D	0	0	I168A	69	125	D150A	131	81	N227A	72	28
A113E	0	0	I168D	0	0	D150E	128	228	N227D	11	0
A113H	0	0	I168E	0	0	D150H	105	37	N227E	36	0
A113K	0	0	I168H	13	35	D150K	51	0	N227H	19	19
A113R	0	0	I168K	0	0	D150R	44	0	N227K	29	0
F114A	28	8	I168R	0	0	D150W	81	60	N227R	55	0
F114D	0	0	S169A	112	64	Y157A	11	0	V230A	17	0
F114E	0	0	S169D	0	0	Y157D	1	0	V230D	0	0
F114H	18	20	S169E	0	0	Y157E	13	0	V230E	0	0
F114K	0	0	S169H	0	0	Y157H	24	0	V230H	0	0
F114R	0	0	S169K	0	0	Y157K	7	0	V230K	3	0
W115A	0	0	S169R	0	0	Y157R	0	0	V230R	6	12
W115D	0	0	D170A	0	0	G162A	0	0	S234A	88	17
W115E	0	0	D170E	0	0	G162D	0	0	S234D	5	0
W115H	0	0	D170H	0	0	G162E	0	0	S234E	4	7
W115K	0	0	D170K	0	0	G162H	0	0	S234H	32	0
W115R	0	0	D170R	0	0	G162K	0	0	S234K	0	0
						G162R	0	0	S234R	0	0

The casein- and FAGLA-hydrolytic reactions were carried out with the culture supernatant at the concentration of 1.25–5 and 5% (v/v), respectively. The average values of triplicate determination, which are relative to that of the wild-type thermolysin, are indicated.
[a]Casein-hydrolysis (units/ml). [b]FAGLA-hydrolysis (μM).

the variants at 195–260 nm were essentially the same as that of the WT enzyme, suggesting that significant conformational change was not induced in thermolysin by mutation (data not shown).

Hydrolytic Activities of the Variants for Casein, FAGLA and ZDFM—The specific activity of the thermolysin-catalysed hydrolysis of casein at pH 7.5, at 25°C is shown in Table 2. All thermolysin variants can be classified into two groups: the specific activities of six variants were 80–110% of that of WT thermolysin, and those of the other six were 30–60%.

The pH-dependence of k_{cat}/K_m of the thermolysin-catalysed hydrolysis of FAGLA at 25°C is shown in Fig. 3A. The $(k_{cat}/K_m)_o$, pK_{e1} and pK_{e2} values are summarized in Table 3. All plots showed bell-shaped curves with the optimal pH around 7. The $(k_{cat}/K_m)_0$ values of the D150E and I168A variants were 280% and 230% of that of WT thermolysin, respectively and those of the other ten variants were in the range of 10–110%. The pK_{e1} values of the F114H and D150H were 5.7 ± 0.0 and 5.8 ± 0.0, higher by 0.4 ± 0.0 and 0.5 ± 0.0 units, respectively, than that of the WT enzyme. These differences in pK_{e1} are comparable to that (0.4 ± 0.1 units) of the previously reported variant, N112D (*25*). The pK_{e2} values of the F114H and D150H and the pK_{e1} and pK_{e2} values of the other 10 variants were almost identical with those of WT thermolysin.

ZDFM is the substrate to which the Michaelis–Menten kinetics is applicable to determine k_{cat} and K_m separately. The dependence of the initial reaction rate (v_0) of the thermolysin-catalysed hydrolysis of ZDFM at pH 7.5, at 25°C on the substrate concentration is shown in Fig. 3B. All plots showed saturated profiles, and the k_{cat} and K_m values were determined separately (Table 4). The k_{cat}/K_m values of the D150E, D150W, N227H and I168A variants were 280%, 180%, 160% and 140% of that of WT thermolysin, respectively. Their k_{cat} and K_m values were in the range of 160–550% and 110–310% of those of the WT enzyme, respectively. Therefore, the increase in their

Table 2. **Specific activity of the wild-type thermolysin and the variants in the hydrolysis of casein at 25°C.**

Thermolysin	Specific activity	(units/mg)
Wild-type	10800 ± 1900	(1.0)
F114A	11400 ± 700	(1.1)
F114H	3400 ± 100	(0.3)
D150A	8900 ± 600	(0.8)
D150E	9300 ± 200	(0.9)
D150H	8400 ± 1200	(0.8)
D150W	6200 ± 100	(0.6)
I168A	6800 ± 600	(0.6)
I168H	4200 ± 200	(0.4)
S169A	8900 ± 200	(0.8)
N227A	5500 ± 300	(0.5)
N227H	11800 ± 2400	(1.1)
S234A	4200 ± 0	(0.4)
L144S[a]	4900 ± 0	(0.5)
G8C/N60C/S65P/L144S[a]	5400 ± 0	(0.5)

The average of triplicate determination with SD values is shown. Numbers in parentheses indicate the values relative to the wild-type thermolysin. [a]Ref. 21.

Downloaded from http://jb.oxfordjournals.org/ at University of Science and Technology of China on September 28, 2012

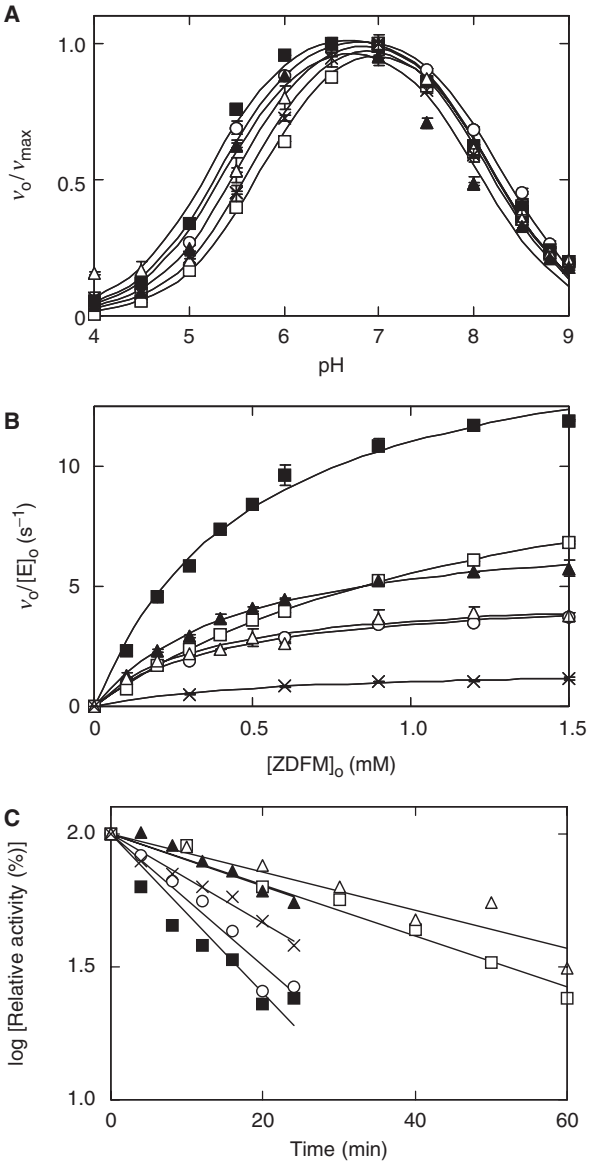

Fig. 3. **Characterization of the thermolysin variants.** (A) Effect of pH on the initial reaction rate (v_o) in the thermolysin-catalysed hydrolysis of FAGLA. The reaction was carried out with the initial concentrations of enzyme and FAGLA of 25–400 nM and 400 μM, respectively, at 25°C. The v_o observed at the optimal pH is denoted by v_{max}. (B) Dependence on the substrate concentration of v_o in the thermolysin-catalysed hydrolysis of ZDFM. The reaction was carried out with the initial enzyme concentration ($[E]_o$) of 25–400 nM at 25°C. $v_o/[E]_o$ is plotted against the ZDFM concentration. (C) Thermal inactivation of thermolysins. Thermolysin (0.5–8 μM) in 40 mM HEPES–NaOH (pH 7.5) buffer containing 10 mM $CaCl_2$ was incubated at 80°C for a specified time. The FAGLA-hydrolytic reaction was carried out with the initial concentrations of enzyme and FAGLA of 25–400 nM and 400 μM, respectively, at 25°C. The remaining activity (k_{cat}/K_m) was expressed as the relative value to that [wild-type (WT) thermolysin, 34,000 $M^{-1}s^{-1}$; F114H, 15,000 $M^{-1}s^{-1}$; D150H, 10,000 $M^{-1}s^{-1}$; D150E, 55,000 $M^{-1}s^{-1}$; I168H, 17,000 $M^{-1}s^{-1}$; and I168A, 51,000 $M^{-1}s^{-1}$] of the intact enzyme and plotted against the incubation time. Symbols for the WT and mutated thermolysin variants: WT thermolysin, open circle; F114H, cross; D150H, open square; D150E, closed square; I168H, open triangle; and I168A, closed triangle. Error bars indicate SD values.

k_{cat}/K_m values can be ascribed to the increase in k_{cat} by the mutations. The k_{cat}/K_m values of the other eight variants were in the range of 10–120% of that of WT thermolysin. These results also indicate that, like the previously reported highly active thermolysin variants, L144S and G8C/N60C/S65P/L144S (*21*), the D150E and I168A variants were more active than WT thermolysin in the hydrolysis of both FAGLA and ZDFM.

NaCl-Induced Activation of Thermolysin in the Hydrolysis of FAGLA—We have reported that thermolysin activity increases with increasing concentration of neutral salts such as NaCl and that the degree of the NaCl-induced activation, which is defined as the ratio of the k_{cat}/K_m value at 4 M NaCl to that at 0 M NaCl, is in the range of 13–15 (*18*). Table 5 shows the k_{cat}/K_m values at 0 and 4 M NaCl in the hydrolysis of FAGLA and the degrees of the NaCl-induced activation. The degrees of the activation of the F114A, F114H and D150W variants were in the range of 120–130% of that of WT thermolysin. Those of the D150E and I168A were in the range of 60–70% of that of the WT enzyme, which is almost comparable to that of the thermolysin G8C/N60C/S65P/L144S variant (40%) (*21*). Those of the other seven variants were in the range of 60–100% of that of the WT enzyme.

Thermal Stability of Thermolysin Variants—Figure 3C shows the time-dependence of the thermal inactivation of the thermolysin variants at 80°C. The inactivation followed pseudo-first-order kinetics. The observed first-order rate constants, k_{obs}, for the thermal inactivation of WT thermolysin and its variants are summarized in Table 6. The k_{obs} values of the following seven variants, D150H, D150W, I168A, I168H, N227A, N227H and S234A, were in the range of 30–50% of that of WT thermolysin, indicating that the stability of these variants were much improved. The k_{obs} values of the other five variants were in the range of 70–120% of that of the WT. Taken together, the thermolysin I168A variant, like the G8C/N60C/S65P/L144S (*21*), has higher activity and stability than WT thermolysin.

DISCUSSION

Role of Each Polypeptide Region in the Active Site of Thermolysin—In this study, various mutations were introduced into polypeptide regions at the active site of thermolysin. Most of the mutations (>80%) at the N-terminal sheet and α-helix 2 regions abolished the hydrolytic activities for casein and FAGLA while considerable numbers of mutations (about 40%) at the C-terminal loops 1 and 2 abolished the activity for FAGLA, but retained that for casein (Table 1). The results provide the catalytic role of each polypeptide region in the active site of thermolysin: the N-terminal sheet and α-helix 2 are critical in catalysis and the C-terminal loops 1 and 2 are ciritcal in substrate recognition.

The α-helix 2 (Ala163–Val176) is the longest α-helix in thermolysin, stretching from the active site to the molecular surface of the other side. The active sites of *Streptomyces caespitosus* neutral protease (ScNP) and human matrix metalloproteinase 7 (matrilysin or MMP-7), the small metalloproteinases with molecular

Downloaded from http://jb.oxfordjournals.org/ at University of Science and Technology of China on September 28, 2012

Table 3. **pK_e values and intrinsic k_{cat}/K_m [$(k_{cat}/K_m)_0$] of the wild-type thermolysin and the variants in the hydrolysis of FAGLA at 25°C.**

Thermolysin	pK_{e1}	pK_{e2}	$(k_{cat}/K_m)_o \times 10^{-4}$ ($M^{-1}s^{-1}$)
Wild-type	5.3 ± 0.0 (0.0)	8.3 ± 0.0 (0.0)	4.0 ± 0.1 (1.0)
F114A	5.0 ± 0.1 (–0.3)	8.4 ± 0.1 (+0.1)	0.7 ± 0.0 (0.2)
F114H	5.7 ± 0.0 (+0.4)	8.1 ± 0.0 (–0.2)	2.0 ± 0.0 (0.5)
D150A	5.1 ± 0.1 (–0.2)	8.0 ± 0.1 (–0.3)	3.8 ± 0.1 (1.0)
D150E	5.2 ± 0.1 (–0.1)	8.2 ± 0.0 (–0.1)	11.0 ± 0.0 (2.8)
D150H	5.8 ± 0.0 (+0.5)	8.2 ± 0.0 (–0.1)	1.6 ± 0.0 (0.4)
D150W	5.1 ± 0.1 (–0.2)	8.1 ± 0.1 (–0.2)	2.8 ± 0.1 (0.7)
I168A	5.4 ± 0.1 (+0.1)	8.1 ± 0.1 (–0.2)	9.1 ± 0.4 (2.3)
I168H	5.5 ± 0.1 (+0.2)	8.2 ± 0.1 (–0.1)	4.4 ± 0.1 (1.1)
S169A	5.5 ± 0.0 (+0.2)	8.3 ± 0.0 (0.0)	2.7 ± 0.1 (0.7)
N227A	5.2 ± 0.1 (–0.1)	8.4 ± 0.1 (+0.1)	1.5 ± 0.1 (0.4)
N227H	5.3 ± 0.0 (0.0)	8.4 ± 0.0 (+0.1)	4.1 ± 0.1 (1.0)
S234A	5.2 ± 0.1 (–0.1)	8.1 ± 0.1 (–0.2)	0.4 ± 0.0 (0.1)
N112D[a]	5.7 ± 0.1 (+0.4)	8.1 ± 0.0 (–0.2)	2.4 ± 0.0 (0.6)
L144S[b]	5.2 ± 0.1 (–0.1)	8.5 ± 0.1 (+0.2)	22.2 ± 0.7 (5.6)
G8C/N60C/ S65P/L144S[b]	5.3 ± 0.4 (0.0)	8.3 ± 0.1 (0.0)	24.7 ± 0.7 (6.2)

The average of triplicate determination with SD values is shown. Numbers in parentheses indicate ΔpK_e compared to the wild-type thermolysin and the $(k_{cat}/K_m)_o$ relative to the wild-type thermolysin. [a]Ref. 25. [b]Ref. 21.

Table 4. **Kinetic parameters of the wild-type thermolysin and the variants in the hydrolysis of ZDFM at 25°C.**

Thermolysin	K_m (mM)	k_{cat} (s^{-1})	k_{cat}/K_m ($mM^{-1}s^{-1}$)
Wild-type	0.40 ± 0.03 (1.0)	4.8 ± 0.1 (1.0)	11.9 ± 0.7 (1.0)
F114A	0.31 ± 0.07 (0.8)	0.8 ± 0.1 (0.2)	2.4 ± 0.4 (0.2)
F114H	0.56 ± 0.11 (1.4)	1.6 ± 0.1 (0.3)	2.9 ± 0.3 (0.2)
D150A	1.28 ± 0.08 (3.2)	14.0 ± 0.5 (2.9)	11.0 ± 0 (0.9)
D150E	0.50 ± 0.05 (1.3)	16.5 ± 0.7 (3.4)	33.1 ± 2.1 (2.8)
D150H	1.34 ± 0.06 (3.4)	13.0 ± 0.4 (2.7)	9.7 ± 0.2 (0.8)
D150W	1.24 ± 0.07 (3.1)	26.1 ± 0.8 (5.4)	21.1 ± 0.5 (1.8)
I168A	0.46 ± 0.03 (1.2)	7.7 ± 0.2 (1.6)	16.8 ± 0.7 (1.4)
I168H	0.35 ± 0.06 (0.9)	4.8 ± 0.3 (1.0)	13.8 ± 1.6 (1.2)
S169A	0.44 ± 0.04 (1.1)	3.2 ± 0.1 (0.7)	7.3 ± 0.4 (0.6)
N227A	0.91 ± 0.27 (2.3)	3.0 ± 0.5 (0.6)	3.3 ± 0.5 (0.3)
N227H	0.53 ± 0.07 (1.3)	10.0 ± 0.6 (2.1)	19.1 ± 1.5 (1.6)
S234A	0.57 ± 0.04 (1.4)	0.4 ± 0.0 (0.1)	0.8 ± 0.0 (0.1)
L144S[a]	0.06 ± 0.04 (0.2)	6.7 ± 0.5 (1.4)	112 ± 14 (9.4)
G8C/N60C/ S65P/L144S[a]	0.10 ± 0.05 (0.3)	7.0 ± 0.5 (1.5)	70 ± 14 (5.9)

The average of triplicate determination with SD value is shown. Numbers in parentheses indicate values relative to the wild-type thermolysin. [a]Ref. 21.

Table 5. **Degree of salt-induced activation of the wild-type thermolysin and the variants in the hydrolysis of FAGLA at 25°C.**

Thermolysin	$k_{cat}/K_m \times 10^{-4}$ ($M^{-1}s^{-1}$)		(B/A)
	0 M NaCl (A)	4 M NaCl (B)	
Wild-type	3.1 ± 0.0 (1.0)	51 ± 2 (1.0)	16 (1.0)
F114A	0.4 ± 0.0 (0.1)	8 ± 0 (0.2)	19 (1.2)
F114H	1.5 ± 0.0 (0.5)	31 ± 3 (0.6)	20 (1.3)
D150A	2.4 ± 0.1 (0.8)	35 ± 2 (0.7)	15 (0.9)
D150E	7.4 ± 0.1 (2.4)	67 ± 0 (1.3)	9 (0.6)
D150H	1.3 ± 0.0 (0.4)	20 ± 1 (0.4)	16 (1.0)
D150W	1.8 ± 0.1 (0.6)	37 ± 2 (0.7)	21 (1.3)
I168A	7.0 ± 0.2 (2.3)	79 ± 6 (1.5)	11 (0.7)
I168H	3.0 ± 0.2 (1.0)	41 ± 5 (0.8)	13 (0.8)
S169A	2.2 ± 0.1 (0.7)	27 ± 1 (0.5)	13 (0.8)
N227A	1.2 ± 0.1 (0.4)	16 ± 1 (0.3)	13 (0.8)
N227H	3.1 ± 0.1 (1.0)	49 ± 1 (1.0)	16 (1.0)
S234A	0.3 ± 0.0 (0.1)	3 ± 0 (0.1)	10 (0.6)
G8C/N60C/ S65P/L144S[a]	19.2 ± 0.4 (6.2)	138 ± 1 (2.7)	7 (0.4)

The reaction was carried out in 40 mM HEPES–NaOH buffer at pH 7.5 containing 10 mM $CaCl_2$, at 25°C. The average of triplicate determination with SD value is shown. Numbers in parentheses indicate values relative to the wild-type thermolysin. [a]Ref. 21.

Table 6. **Thermal stability of the wild-type thermolysin and the variants.**

Thermolysin	k_{obs}[a] $\times 10^4$ (s^{-1})	
Wild-type	8.3 ± 1.0	(1.0)
F114A	8.6 ± 1.1	(1.0)
F114H	6.2 ± 0.4	(0.7)
D150A	9.2 ± 0.3	(1.1)
D150E	10.1 ± 0.9	(1.2)
D150H	4.0 ± 0.2	(0.5)
D150W	4.0 ± 0.3	(0.5)
I168A	4.5 ± 0.3	(0.5)
I168H	2.9 ± 0.4	(0.3)
S169A	5.7 ± 0.6	(0.7)
N227A	3.0 ± 0.2	(0.4)
N227H	3.4 ± 0.3	(0.4)
S234A	3.0 ± 0.2	(0.4)
L144S[b]	8.6 ± 0.6	(1.0)
G8C/N60C/S65P/L144S[b]	4.7 ± 0.5	(0.6)
S53D[c]	4.6 ± 0.2	(0.6)

[a]k_{obs} is the observed first-order rate constant for the thermal inactivation at 80°C. The average of triplicate determination with SD value is shown. Numbers in parentheses indicate values relative to the wild-type thermolysin. [b]Ref. 21. [c]Ref. 24.

masses of 14 and 19 kDa, respectively, do not have such α-helix as the α-helix 2 of thermolysin, and thus their active sites are formed with shallow clefts (*35*) while that of thermolysin is with a deep cleft. Glu166 chelates the catalytic zinc ion, but the roles of other residues in the α-helix 2 have not been known. Our results suggest that introduction of charges at the α-helix 2 may change the position of this α-helix and alter the active-site electrostatic geometry, resulting in the loss of the activity in most of the variants

The N-terminal sheet (Asn112–Trp115) forms the S2′, S1′ and S2 subsites at the active site [the subsites and the corresponding residues in the substrates were designated based upon the nomenclature of Schechter, I. and Berger, A. (*36*)]. Crystallographic studies (*37–39*) have proposed the hydrogen bonds between the atoms in the N-terminal sheet and substrate, which are ND2 of Asn112 and O of the P2′ residue, OD1 of Asn112 and N of the P2′ residue, O of Ala113 and N of the P1′ residue, N of Trp115 and O of the P2 residue, and O of Trp115 and N of the P2 residue.

Downloaded from http://jb.oxfordjournals.org/ at University of Science and Technology of China on September 28, 2012

Our results suggest that these hydrogen bonds are crucial for the activity and are easily affected by the mutation at the N-terminal sheet. In other words, the side chains of the N-terminal sheet determine the structure of the protein backbone which enables the substrate to bind the active site. Our results are also consistent with our previous result that the mutation of Tyr115 into aromatic residues, Phe or Tyr, did not affect much, but that into Val or Leu abolished the activity (*40*).

The C-terminal loops 1 (Asp150–Gly162) and 2 (Gln225–Ser234) are located on the other side of the N-terminal sheet. The former connects the α-helices 1 and 2. Our results suggest that these two regions are responsible for substrate specificity; however, such property has not been reported. The relative K_m values of the variants at Asp150, Asn227 and Ser234 to that of WT thermolysin in the hydrolysis of ZDFM were in the range of 1.3–3.4, suggesting that these residues are involved in the ZDFM recognition. However, it has been reported that these residues are not involved in the substrate recognition by crystallographic studies. For example, in the complexes of thermolysin with its representative inhibitors *N*-(α-L-rhamnopyranosyloxyhydroxyphosphinyl)-L-leucyl-L-tryptophan (phosphoramidon) or *N*-phosphoryl-L-leucinamide (*P*-Leu-NH_2), the side chain of the P1′ residue, Leu, is accommodated in the space formed by several residues such as Phe130, Val139 and Leu199 and that the rhamnosyl moiety, which corresponds to the P1 residue, does not interact with any residues of thermolysin (*41*). This crystallographic study suggests that neither residue in the C-terminal loops 1 and 2 are involved in the substrate recognition. Accordingly, we speculate that some residues at the C-terminal loops 1 and 2 may move during catalysis so to interact with substrate. It should also be noted that Tyr157 has been believed to stabilize the transition state based on the crystallographic studies (*37–39*). However, five out of six variants with the mutation at Tyr157 retained the activity although it is much lower than that of WT thermolysin (Table 1).

Modifying the pH-dependence of Thermolysin by Site-Directed Mutagenesis—The mutations of Phe114 and Asp150 into histidine residues resulted in an increase in pK_{e1} by 0.4 and 0.5 units, respectively (Table 2). However, the results are contradictory to our hypothesis that introduction of a positive charge into the active site may shift the optimal pH to the acidic side by suppressing the protonation of the ionizing residue responsible for pK_{e1}, which may be assigned to Glu143 or the zinc-bound water (*8*, *18*). This hypothesis is based on our previous result that the mutation of Asn112 to Asp resulted in an increase in pK_{e1} by 0.4 units (*25*). Therefore, the mechanism of the pK_{e1} shift observed in this study is not clear. However, it is interesting to note that the hydrolytic activities (k_{cat}/K_m) of the N112D variant for FAGLA and ZDFM are 60% and 0.2%, respectively, in comparison with those of WT thermolysin, whereas those of the D150H variant are 40% and 80%, respectively. FAGLA is a neutral substrate while ZDFM is negatively charged. The relative values of the ZDFM-hydrolytic activities of the N112D and D150H compared to their FAGLA-hydrolytic activities are 0.0033 and 2.0, respectively, suggesting that the introduced negative and positive charges at the positions 112 and 150, respectively, affect not only the protonation of the ionizing residue responsible for pK_{e1} but also the recognition of the side chain of the P1 residue of the substrate.

Improving the Activity and Stability of Thermolysin by Site-directed Mutagenesis—Taken together the results previously reported (*16*, *21–24*) and presented in this study, the three single-point mutations of Leu144 to Ser (L144S), Asp150 to Glu (D150E) and Ile168 to Ala (I168A) increase thermolysin activity; the triple-point mutation G8C/N60C/S65P and three single-point mutations S53D, L155A and I168A increase the stability. Leu144 and Ile168 lie in the α-helices 1 and 2, respectively, and are buried in the interior of the protein. We speculate the mutations L144S and I168A increase the flexibility of thermolysin by decreasing the density of the inner part of the molecule. The activation mechanism of the mutation D150E is not clear. However, it is interesting to note that, in casein hydrolysis, the specific activities of the L144S and I168A variants are 50% and 60%, respectively, of that of WT thermolysin, but that of D150E is 90%, indicating that the mutations L144S and I168A decrease the hydrolytic activity for protein substrates while the mutation of D150E hardly affects it. Such decrease in the proteolytic activity is observed in other mutations (Fig. 4). Although the correlation between the activities for two dipeptidyl substrates, FAGLA and ZDFM, was considerably strong ($r = 0.84$), the correlation between those for FAGLA and casein was weak ($r = 0.20$).

It has been suggested that the salt-induced activation of thermolysin results from combination of two effects, namely, the decrease in dielectric constant of the reaction medium by high concentration of salt and the interaction between ions of salt and charges on the surface of the enzyme (*14*, *17–20*). Weak and negative correlation ($r = -0.54$) was observed between the activity and the degree of the NaCl-induced activation in the hydrolysis of FAGLA (Fig. 4C). However, it is noteworthy that the degree of the activation at x M NaCl of the G8C/N60C/S65P/L144S variant is 1.7^x (*21*), and this value is comparable to that (1.9^x) of WT thermolysin (*18*), suggesting that the salt-induced activation cannot be replaced by introducing mutations into the active site. To explore the mechanism of the salt-induced activation, crystallographic analysis of thermolysin in the presence of 4 M NaCl is currently underway, and we recently reported the preliminary results (*42*).

Stabilization of thermolysin by the mutation G8C/N60C/S65P might be due to the introduction of a disulfide bridge between the positions 8 and 60, and that by the mutation S53D due to the statistic interaction between Lys45 and the introduced Asp53. These effects may restrict unfolding of the surface loop (residues 55–69) and stabilize the Ca^{2+} ion bound at the Ca^{2+}-binding site III (*43*). Stabilization by the mutation L155A might be due to suppressing the autodegradation observed at the peptide bond between Gly154-Leu155 in WT thermolysin (*22*, *23*). On the other hand, the stabilizing mechanism of the mutations D150H, D150W, I168A, I168H, N227A, N227H and S234A is not clear. However, weak correlation ($r = 0.51$) was observed between the specific activity in casein hydrolysis and the first-order rate constant,

Downloaded from http://jb.oxfordjournals.org/ at University of Science and Technology of China on September 28, 2012

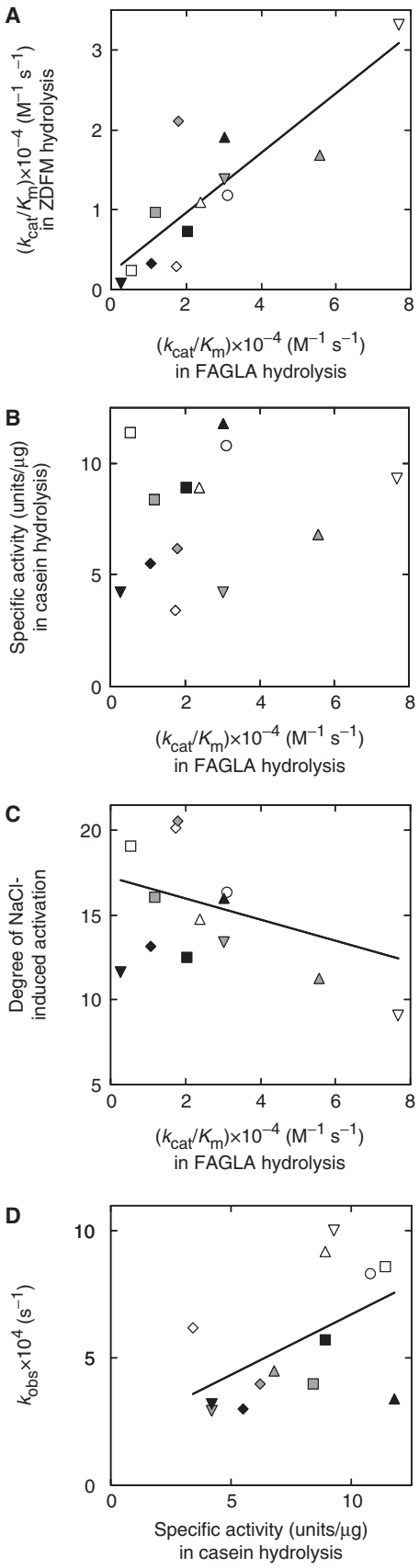

Fig. 4. **Comparison of the activity, stability and the degree of NaCl-induced activation of the thermolysin variants.** (A) Comparison of the ZDFM-hydrolytic activity with the FAGLA-hydrolytic activity. (B) Comparison of the casein-hydrolytic activity with the FAGLA-hydrolytic activity. (C) Comparison of the degree of NaCl-induced activation at 4 M NaCl in the hydrolysis of FAGLA with the FAGLA-hydrolytic activity. (D) Comparison of the first-order rate constant, k_{obs}, of the thermal inactivation at 80°C with the casein-hydrolytic activity. The values of the casein-, FAGLA- and ZDFM-hydrolytic activities at pH 7.5, the degree of NaCl-induced activation at 4 M NaCl in the hydrolysis of FAGLA at pH 7.5, and the k_{obs} of the thermal inactivation at 80°C for WT thermolysin and its 12 variants are cited from Tables 2, 3, 4, 5 and 6, respectively. Symbols for the wild-type (WT) and mutated thermolysin variants: WT thermolysin, open circle; F114A, open square; F114H, open diamond; D150A, open triangle; D150E, open inverted triangle; D150H, grey square; D150W, grey diamond; I168A, grey triangle; I168H, grey inverted triangle; S169A, closed square; N227A, closed diamond; N227H, closed triangle; and S234A, closed inverted triangle. The lines are drawn by the linear least-squares-regression. The regression coefficient, *r*, is: (A) 0.84; (B) 0.20; (C) −0.54; and (D) 0.51.

k_{obs}, observed for the thermal inactivation at 80°C (Fig. 4D). It is generally known that there is a compromise between activity and stability for various enzymes (*44*, *45*). Indeed, the specific activity and the k_{obs} value of the I168A variant were 60% and 50% of those of WT thermolysin, respectively (Tables 2 and 6). Such a property was observed in the D150A and D150E variants, both of which did not display a drop in the activity of casein hydrolysis (Table 2). Interestingly, the specific activity in casein hydrolysis and the k_{obs} value of the N227H variant were 110% and 40% of those of WT thermolysin, respectively (Tables 2 and 6). It also exhibited 1.6-fold higher ZDFM-catalytic activity than WT thermolysin (Table 4), which is coincident with the previous reports (*16*, *21*), suggesting that the mutation Asn227→His is effective to improve the performance of thermolysin. Regarding the activity and stability of thermolysin, it should be noted that we found the activation-and-inhibition dual effects of cobalt ion on thermolysin. Cobalt ion activates thermolysin by replacing the catalytic Zn^{2+} ion but it also destabilizes thermolysin by replacing the Ca^{2+} ions functioning for structural stability. Thus, thermolysin is easily inactivated by autodegradation in the presence of Co^{2+}, although it can be suppressed by the addition of higher concentration of Ca^{2+} ion probably by stabilizing the Ca^{2+}-binding sites (*46*, *47*).

In this study, some thermolysin variants which were improved in activity and/or stability or modified in the pH-activity profile were obtained. Although rational design of enzyme based on the structural data or the computer modeling was anticipated, it is now generally known that the results of mutagenesis study are unpredictable. Indeed, site-directed mutagenesis study of subtilisin BPN′ (composed of 275 amino-acid residues) has been done at almost every amino-acid residue to generate the enzyme of industrial use (*48*). The same approach has been applied also to lysozyme (*49*). In thermolysin, the combination of the mutations should be an attractive strategy for further improving its activity and stability. Mutational effects on enzymes are non-additive, in some

Downloaded from http://jb.oxfordjournals.org/ at University of Science and Technology of China on September 28, 2012

cases (*50*, *51*). However, we previously demonstrated that the single-point mutation of L144S and the triple-point one G8C/N60C/S65P are independent (*21*). Study with the mutational combination will provide not only extremely active and stable thermolysin variants but also a clue useful for understanding the catalytic mechanism, thermostability and halophilicity of thermolysin.

FUNDING

This study was supported in part (K. I.) by Grants-in-Aid for Scientific Research (Nos. 17380065 and 20380061) from the Japan Society for the Promotion of Science.

CONFLICT OF INTEREST

None declared.

REFERENCES

1. Endo, S. (1962) Studies on protease produced by thermophilic bacteria. *J. Ferment. Technol.* **40**, 346–353
2. van den Burg, B. and Eijsink, V.G. (2004) Thermolysin in *Handbook of Proteolytic Enzymes*, 2nd ed. (Barrett, J.A., Rawlings, N.D., and Woessner, J.F., eds.) Vol. 1, pp. 374–387, Elsevier, Amsterdam
3. Inouye, K. (2003) Thermolysin in *Handbook of Food Enzymology* (Whitaker, J.R., Voragen, A.G.J., and Wong, D.W.S., eds.) pp. 1019–1028, Marcel Dekker, New York
4. Latt, S.A., Holmquist, B., and Vallee, B.L. (1969) Thermolysin: a zinc metalloenzyme. *Biochem. Biophys. Res. Commun.* **37**, 333–339
5. Feder, J., Garrett, L.R., and Wildi, B.S. (1971) Studies on the role of calcium in thermolysin. *Biochemistry* **10**, 4552–4556
6. Tajima, M., Urabe, I., Yutani, K., and Okada, H. (1976) Role of calcium ions in the thermostability of thermolysin and *Bacillus subtilis* var. *amylosacchariticus* neutral protease. *Eur. J. Biochem.* **64**, 243–247
7. Morihara, K. and Tsuzuki, H. (1970) Thermolysin: kinetic study with oligopeptides. *Eur. J. Biochem.* **15**, 374–380
8. Inouye, K., Lee, S.-B., and Tonomura, B. (1996) Effect of amino acid residues at the cleavable site of substrates on the remarkable activation of thermolysin by salts. *Biochem. J.* **315**, 133–138
9. Titani, K., Hermodson, M.A., Ericsson, L.H., Walsh, K.A., and Neurath, H. (1972) Amino-acid sequence of thermolysin. *Nature* **238**, 35–37
10. Holmes, M.A. and Matthews, B.W. (1982) Structure of thermolysin refined at 1.6 Å resolution. *J. Mol. Biol.* **160**, 623–639
11. Hangauer, D.G., Monzingo, A.F., and Matthews, B.W. (1984) An interactive computer graphics study of thermolysin-catalyzed peptide cleavage and inhibition by *N*-carboxymethyl dipeptides. *Biochemistry* **23**, 5730–5741
12. Mock, W.L. and Aksamawati, M. (1994) Binding to thermolysin of phenolate-containing inhibitors necessitates a revised mechanism of catalysis. *Biochem. J.* **302**, 57–68
13. Oyama, K., Kihara, K., and Nonaka, Y. (1981) On the mechanism of the action of thermolysin: kinetic study of the thermolysin-catalysed condensation reaction of *N*-benzyloxycarbonyl-L-aspartic acid with L-phenylalanine methyl ester. *J. Chem. Soc. Perkin II,* 356–360
14. Inouye, K. (1992) Effects of salts on thermolysin: activation of hydrolysis and synthesis of *N*-carbobenzoxy-L-aspartyl-L-phenylalanine methyl ester, and a unique change in the absorption spectrum of thermolysin. *J. Biochem.* **112**, 335–340
15. Inouye, K., Kusano, M., Hashida, Y., Minoda, M., and Yasukawa, K. (2007) Engineering, expression, purification, and production of recombinant thermolysin. *Biotechnol. Annu. Rev.* **13**, 43–64
16. Hanzawa, S. and Kidokoro, S. (1999) Thermolysin. in *Encyclopedia of Bioprocess Technology: Fermentation, Biocatalysis, and Bioseparation* (Flickinger, M.C. and Drew, S.W., eds.) pp. 2527–2535, John Wiley & Sons, New York
17. Inouye, K., Kuzuya, K., and Tonomura, B. (1998) Sodium chloride enhances markedly the thermal stability of thermolysin as well as its catalytic activity. *Biochim. Biophys. Acta.* **1388**, 209–214
18. Inouye, K., Lee, S.-B., Nambu, K., and Tonomura, B. (1997) Effects of pH, temperature, and alcohols on remarkable activation of thermolysin by salts. *J. Biochem.* **122**, 358–364
19. Oneda, H., Muta, Y., and Inouye, K. (2004) Substrate-dependent activation of thermolysin by salt. *Biosci. Biotechnol. Biochem.* **68**, 1811–1813
20. Inouye, K., Kuzuya, K., and Tonomura, B. (1998) Effect of salts on the solubility of thermolysin: a remarkable increase in the solubility as well as the activity by the addition of salts without aggregation or dispersion of thermolysin. *J. Biochem.* **123**, 847–852
21. Yasukawa, K. and Inouye, K. (2007) Improving the activity and stability of thermolysin by site-directed mutagenesis. *Biochim. Biophys. Acta.* **1774**, 1281–1288
22. Matsumiya, Y., Nishikawa, K., Aoshima, H., Inouye, K., and Kubo, M. (2004) Analysis of autodegradation sites of thermolysin and enhancement of its thermostability by modifying Leu155 at an autodegradation site. *J. Biochem.* **135**, 547–553
23. Matsumiya, Y., Nishikawa, K., Inouye, K., and Kubo, M. (2005) Mutational effect for stability in a conserved region of thermolysin. *Lett. Appl. Microbiol.* **40**, 329–334
24. Takita, T., Aono, T., Sakurama, H., Itoh, T., Wada, T., Minoda, M., Yasukawa, K., and Inouye, K. (2008) Effects of introducing negative charges into the molecular surface of thermolysin by site-directed mutagenesis on its activity and stability. *Biochim. Biophys. Acta.* **1784**, 481–488
25. Kusano, M., Yasukawa, K., Hashida, Y., and Inouye, K. (2006) Engineering of the pH-dependence of thermolysin activity as examined by site-directed mutagenesis of Asn112 located at the active site of thermolysin. *J. Biochem.* **139**, 1017–1023
26. Tatsumi, C., Hashida, Y., Yasukawa, K., and Inouye, K. (2007) Effects of site-directed mutagenesis of the surface residues Gln128 and Gln225 of thermolysin on its catalytic activity. *J. Biochem.* **141**, 835–842
27. O'Donohue, M.J., Roques, B.P., and Beaumont, A. (1994) Cloning and expression in *Bacillus subtilis* of the *npr* gene from *Bacillus thermoproteolyticus* Rokko coding for the thermostable metalloprotease thermolysin. *Biochem. J.* **300**, 599–603
28. Inouye, K., Minoda, M., Takita, T., Sakurama, H., Hashida, Y., Kusano, M., and Yasukawa, K. (2006) Extracellular production of recombinant thermolysin expressed in *Escherichia coli*, and its purification and enzymatic characterization. *Protein Expr. Purif.* **46**, 248–255
29. Yasukawa, K., Kusano, M., and Inouye, K. (2007) A new method for the extracellular production of recombinant thermolysin by co-expressing the mature sequence and pro-sequence in *Escherichia coli*. *Protein Eng. Des. Sel.* **20**, 375–383
30. Feder, J. (1968) A spectrophotometric assay for neutral protease. *Biochem. Biophys. Res. Commun.* **32**, 326–332
31. Yasukawa, K., Kusano, M., Nakamura, K., and Inouye, K. (2006) Characterization of Gly-D-Phe, Gly-L-Leu, and D-Phe as affinity ligands to thermolysin. *Protein Expr. Purif.* **46**, 332–336

Downloaded from http://jb.oxfordjournals.org/ at University of Science and Technology of China on September 28, 2012

32. Laemmli, U.K. (1970) Cleavage of structural proteins during the assembly of the head of bacteriophage T4. *Nature* **227**, 680–685
33. Sakoda, M. and Hiromi, K. (1976) Determination of the best-fit values of kinetic parameters of the Michaelis-Menten equation by the method of least squares with Taylor expansion. *J. Biochem.* **80**, 547–555
34. Eijsink, V.G., van den Burg, B., Vriend, G., Berendsen, H.J., and Venema, G. (1991) Thermostability of *Bacillus subtilis* neutral protease. *Biochem. Int.* **24**, 517–525
35. Inouye, K., Shimada, T., and Yasukawa, K. (2007) Effects of neutral salts and alcohols on the activity of *Streptomyces caespitosus* neutral protease. *J. Biochem.* **142**, 317–324
36. Schechter, I and Berger, A. (1967) On the size of the active site in proteases. I. papain. *Biochem. Biophys. Res. Commun.* **27**, 157–162
37. Holland, D.R., Tronrud, D.E., Pley, H.W., Flaherty, K.M., Stark, W., Jansonius, J.N., McKay, D.B., and Matthews, B.W. (1992) Structural comparison suggests that thermolysin and related neutral proteases undergo hinge-bending motion during catalysis. *Biochemistry* **31**, 11310–11316
38. Matthews, B.W. (1988) Structural basis of the action of thermolysin and related zinc peptidases. *Acc. Chem. Res.* **21**, 333–340
39. Pelmenschikov, V., Blomberg, M.R., and Siegbahn, P.E. (2002) A theoretical study of the mechanism for peptide hydrolysis by thermolysin. *J. Biol. Inorg. Chem.* **7**, 284–298
40. Inouye, K., Mazda, N., and Kubo, M. (1998) Need for aromatic residue at position 115 for proteolytic activity found by site-directed mutagenesis of tryptophan 115 in thermolysin. *Biosci. Biotechnol. Biochem.* **62**, 798–800
41. Tronrud, D.E., Monzingo, A.F., and Matthews, B.W. (1986) Crystallographic structural analysis of phosphoramidates as inhibitors and transition-state analogs of thermolysin. *Eur. J. Biochem.* **157**, 261–268
42. Kamo, M., Inouye, K., Nagata, K., and Tanokura, M. (2005) Preliminary X-ray crystallographic analysis of thermolysin in the presence of 4 M NaCl. *Acta. Cryst.* **D61**, 710–712
43. Durrschmidt, P., Mansfeld, J., and Ulbrich-Hofmann, R. (2005) An engineered disulfide bridge mimics the effect of calcium to protect neutral protease against local unfolding. *FEBS J.* **272**, 1523–1534
44. Yutani, K., Ogasahara, K., Tsujita, T., and Sugino, Y. (1987) Dependence of conformational stability on hydrophobicity of the amino acid residue in a series of variant proteins substituted at a unique position of tryptophan synthase α subunit. *Proc. Natl Acad. Sci. USA* **84**, 4441–4444
45. Shoichet, B.K., Baase, W.A., Kuroki, R., and Matthews, B.W. (1995) A relationship between protein stability and protein function. *Proc. Natl Acad. Sci. USA* **92**, 452–456
46. Hashida, Y. and Inouye, K. (2007) Kinetic analysis of the activation-and-inhibition dual effects of cobalt ion on thermolysin activity. *J. Biochem.* **141**, 843–853
47. Hashida, Y. and Inouye, K. (2007) Molecular mechanism of the inhibitory effect of cobalt ion on thermolysin activity and the suppressive effect of calcium ion on the cobalt ion-dependent inactivation of thermolysin. *J. Biochem.* **141**, 879–888
48. Cherry, J.R. and Fidantsef, A.L. (2003) Directed evolution of industrial enzymes: an update. *Curr. Opin. Biotechnol.* **14**, 438–443
49. Matthews, B.W. (1996) Structural and genetic analysis of the folding and function of T4 lysozyme. *FASEB J.* **10**, 35–41
50. LiCata, V.J. and Ackers, G.K. (1995) Long-range, small magnitude nonadditivity of mutational effects in proteins. *Biochemistry* **34**, 3133–3139
51. de Kreij, A., van den Burg, B., Venema, G., Vriend, G., Eijsink, V.G., and Nielsen, J.E. (2002) The effects of modifying the surface charge on the catalytic activity of a thermolysin-like protease. *J. Biol. Chem.* **277**, 15432–15438

Downloaded from http://jb.oxfordjournals.org/ at University of Science and Technology of China on September 28, 2012